DOI: 10.1111/tgis.12788

RESEARCH ARTICLE

Transactions in GIS WILEY

Analyzing routes in Ottoman Greater Syria using historical GIS: The 1849 Saida map

Motti Zohar[1] | Yuval Ben-Bassat[2]

[1]Department of Geography and Environmental Studies, University of Haifa, Haifa, Israel

[2]Department of Middle Eastern and Islamic Studies, University of Haifa, Haifa, Israel

Correspondence
Motti Zohar, Department of Geography and Environmental Studies, University of Haifa, Abba Khoushy Ave 199, Haifa 3498838, Israel.
Email: mzohar@geo.haifa.ac.il

Abstract

Ottoman cartographic materials are important sources of information on 19th and early 20th-century Greater Syria. However, large portions of this corpus have yet to be examined. This study explores a rare mid-19th-century Ottoman map of the Province of Saida preserved in the Ottoman Archive in Istanbul. It lists travel times between villages, towns, and administrative centers in Greater Syria under Ottoman rule, and shows the network of routes connecting these localities. Using an historical GIS approach, we evaluated the characteristics of the map and its cartographical accuracy and merits. The network of routes on the map is compared to route reconstructions based on least-cost-path principles. The discussion focuses on the historical context of the map and the ways in which it reflects the strength of Ottoman rule and familiarity with Greater Syria at the time.

1 | INTRODUCTION

Most studies of cartographic materials depicting Greater Syria have examined European efforts to survey this region, which started at the turn of the 19th century (e.g., Ben-Arieh & Bartal, 1983; Goren, 2001; Schelhaas, Faehndrich, & Goren, 2017). By contrast, maps produced by the Ottoman Empire have largely been ignored. Thus, while the literature examining the European cartography of Greater Syria in the 19th century has been accumulating, there is a substantial lack of information about Ottoman cartography. In the last few years, however, there has been increasing interest in Ottoman cartography and the valuable information Ottoman maps may contain about the imperial provinces (Ben-Bassat & Ben-Artzi, 2015, 2016, 2018, 2019; Kark, 2004; Marom, 2018).

GIScience techniques are ideal methods to examine historical maps. In the literature, this line of research is part of the historical GIS (HGIS) sub-field (Bailey & Schick, 2009; Gregory & Ell, 2007; Gregory & Healy, 2007; Knowles, 2005; Zohar, 2020). HGIS has been implemented worldwide in numerous historical travel and

narrative-based studies (e.g., Balletti & Guerra, 2016; Bender, Boehmer, Jens, & Schumacher, 2005; Manzano, Martínez, & San-Antonio-Gomez, 2012), and also for the cartography of Greater Syria (e.g., Anderson, 2019; Cooper & Gregory, 2011; Davie & Frumin, 2007; Lafreniere & Gilliland, 2015; Levin, 2006; Levin, Kark, & Galilee, 2010; Schaffer & Levin, 2014, 2016; Zohar, 2017, 2019). Here we used HGIS techniques to examine a rare mid-19th-century Ottoman map of the Province of Saida (Sidon in modern-day Lebanon), preserved today in the Ottoman Archive in Istanbul (Figure 1). The map provides information about villages, towns, administrative centers, and routes in Greater Syria under Ottoman rule (present-day Syria, Lebanon, Israel, the West Bank, and the Gaza Strip). The cartographer(s) of the map are anonymous, but one can assume that it was drawn up for official Ottoman usage. We evaluated the accuracy and completeness of the map and the routes portrayed on it in light of the historical context and Ottoman imperial policies. This map is intriguing because it raises several questions related to its cartographic characteristics, but also as regards the regional and imperial historical setting at the time: (a) How accurate and inclusive is this map? (b) What are the key characteristics of the Ottoman routes and do they follow least-cost considerations in terms of effort or time spent traveling? (c) What was the original purpose of this map? (d) What can we learn from the map about the historical context of the time?

2 | HISTORICAL BACKGROUND

In 1839, the Ottoman Empire initiated an ambitious set of reforms called the Tanzimat. One of the Empire's key aims was to boost economic activity and strengthen the hold of the central regime over the periphery, which was tenuous at the time. In terms of infrastructure, the Empire had ambitious plans to build new roads and railroads, connect the region to telegraph lines, develop a water infrastructure, and upgrade existing ports. In many cases, however, the Empire lacked the resources to carry out its plans and was obligated to award concessions to foreign companies to construct infrastructure projects in return for a share of the profits from their operation (Ben-Bassat & Ben-Artzi, 2016, 2018). The Ottoman archive contains numerous examples of development projects and concessions granted to foreign companies from the second half of the 19th century.[1]

It took some time before the reforms percolated to the provinces of the Empire; many were merely initialized as a declaration of intent and thus only remained on paper for several years. The Empire only gradually regained control over the region of Greater Syria and could subdue its autonomous regions, especially in the mountainous regions (Schölch, 1993, pp. 182, 197) after the end of the Egyptian crisis in 1840 when the forces loyal to Muhammad ʿAli (the governor of Egypt) took over Greater Syria until the European Powers forced them to withdraw. Thus, the reforms in Greater Syria only began to be felt in earnest after 1860, in their second phase (Abu-Manneh, 1990; Buessow, 2011; Máoz, 1968).

During most of the Ottoman period, Saida (a city in present-day Lebanon, about 45 km south of Beirut) was the capital of the province (*eyalet*) (Figure 2). Toward the end of the 18th century, the provincial capital was moved south to the city of Acre (northern Palestine) by Jazzar Pasha (1722–1804), the governor of the province. In the aftermath of the Egyptian crisis, the capital of the province returned to Saida. Nevertheless, the major city in this province—which was also the commercial hub at the time—was the emerging port city of Beirut.

Not surprisingly, the governor of the province officiated in Beirut, a fact which later led to the establishment of the Province of Beirut in 1888. This newly created province eclipsed Saida Province and controlled territories extending from the border of the Sinai Peninsula (south of Gaza) to the shores of northern Syria (Akarli, 1993; Fawaz, 1984; Hanssen, 2005). The special administrative region of Mount Lebanon, which was set up in 1842, nominally remained under the governor of Saida until 1861. It was divided into a northern and a southern district, bordered by the Beirut–Damascus road. In the aftermath of the civil war in Mount Lebanon and the massacres of Christian populations there and in Damascus in 1860, a special administrative regime under international tutelage was established in this region, called the *mutasarrıfıyya* of Mount Lebanon (Akarli, 1993; Hanssen, 2005).

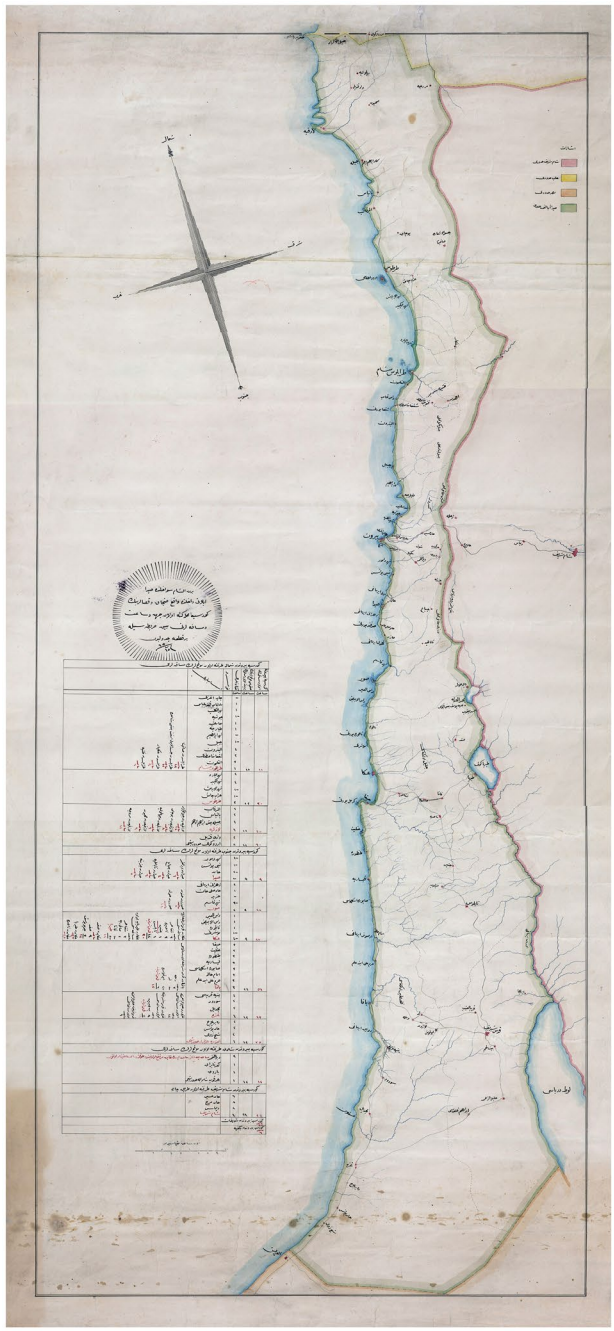

FIGURE 1 Map of the Province of Saida from the Ottoman Archive in Istanbul (*Source*: Başbakanlık Osmanlı Arşivi (BOA), HRT, Map 0520, 15 Şaban 1265 [July 6, 1849]). The table on the left-hand side lists the travel times between settlements, cities, and administrative centers

3 | THE SAIDA MAP

The Saida map, executed on a paper canvas, extends from El-ʿArish (Sinai, Egypt) in the south to Jabal al-Akrad (southern Turkey) in the north. Its title (in a dotted circle above the table of routes) is "A map and timetable

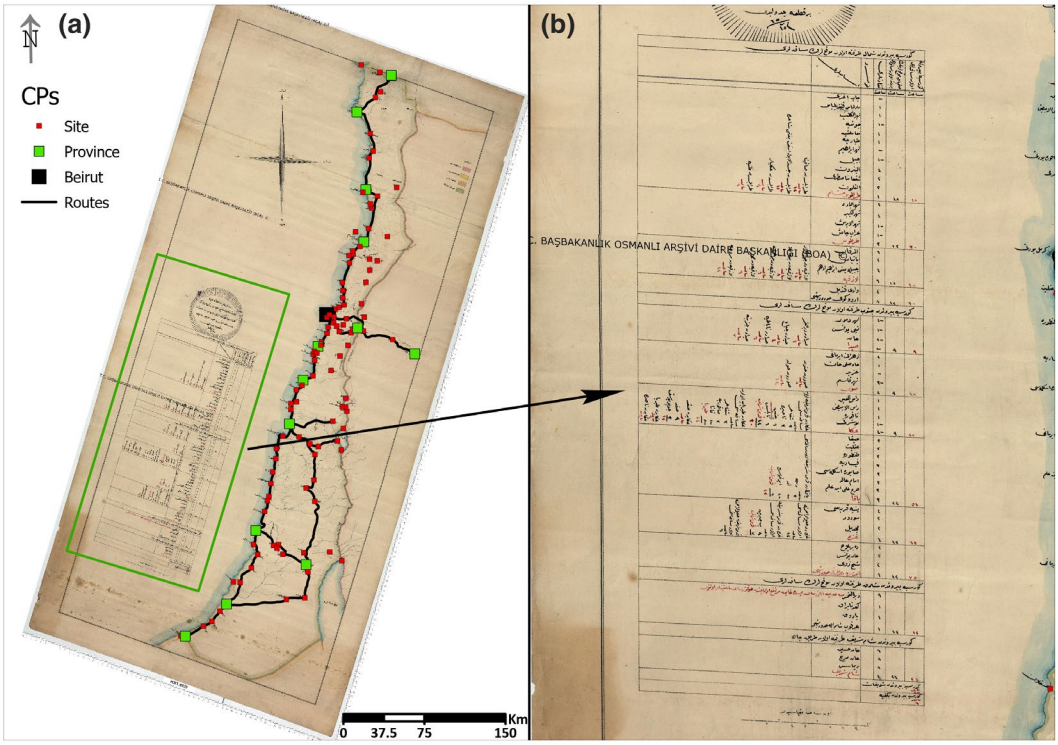

FIGURE 2 (a) The Saida map registered to UTM WGS84 zone 36N. Note the 113 linking CPs categorized into sites, administrative centers, and the city of Beirut (for additional details, see Appendix 1). The digitized routes are outlined in black and the green delineations correspond to the embedded table listing the routes and travel durations. (b) Magnification of the table of routes and travel durations (see English translation in Table 1)

showing the distance, time and direction to the provincial and district centers from Beirut which is located on the shores of Syria in the province of Saida" (Figure 1). The map does not have any graticules, coordinates, or a scale bar, but rather a compass card ("Wind Rose") and a legend indicating the provinces that appears in the upper-left and upper-right corners of the map, respectively. The reddish-pink, yellow, pale orange, and light green in the legend denote the borders of the provinces of Damascus, Halab (Aleppo), Egypt, and Saida, respectively. The map is aligned with the Mediterranean coast, but the compass card points to the north. The map indicates the administrative borders, localities such as villages, towns, and administrative centers, routes between these localities, rivers and streams, and bodies of water including the Hula swamp that was drained later and is practically nonexistent today (Duany, 2012).

A table of distances between the localities appears on the left side of the map. The values are not given in metrics such as kilometers, but rather in terms of travel time. Below the table, a 10-hr ruler is scaled at equal intervals, which probably implies that the scale does not take the topography and terrain into account. The table lists the times on horseback from administrative centers such as Beirut, Saida, Sur, Acre, Jaffa, and Gaza (all marked in red in the table) to other localities along the Mediterranean coast. The riding times from these administrative centers to locations further inland to the east appear vertically (Table 1). The starting point for measuring the travel times to localities along the coast is Beirut, situated at point zero (*kursi*), from which the routes go northwards and southwards. For instance, the total travel time from the administrative center of Jaffa to Acre is listed as 24 hr and the total travel time from Jaffa to Beirut is 51 hr.[2]

TABLE 1 Travel duration timetable in the Saida map (Figure 1). Note that in the columns "Name" and "Distance from the administrative centers to Beirut," the administrative provincial centers are marked in red on the original map, in addition to the travel time indicated next to it. This table is a direct translation of the table on the map that respects the original format (including potential errors, misspellings, etc.)

Name	Number	Total Hours	Distance of provincial centers from each other Hours	Distance from the administrative centers to Beirut Hours
Distances between localities in the North from the Seat in Beirut				
From Trablus to Safita, 12 hr From Trablus to Jisr al-Aboul 12 hr From Trablus to ʿAkyar 9 hr From Trablus to Danniyeh (Sir El Danniyeh) 6 hr	Mouth of River (Beirut)	0.5	18	18
	Deir Mar Elias	1		
	Nahr al-Kalb	1		
	Jounieh	1.5		
	Maʿamaltein	1		
	Tabarja	1		
	Nahr Ibrahim	0.5		
	Jbeil	1.5		
	Batroun	4		
	Chekka	2		
	al-Qalamun	3		
	Trablus Sham	1		
	Nahr al-Barid	2	12	30
	Nahr al-Kabir	4		
	Nahr al-Abrash	1.5		
	ʿArab Jaish	1.5		
	Tartus	3		
From Latakia to Jabl al-Akrad 12 hr From Latakia to Bujak 8 hr From Latakia to Bahluliyya 6 hr From Latakia to Sahbun 6 hr From Latakia to Saruja 12 hr	Al-Marqab	6	18	48
	Banias	2		
	Jablah (Ibrahim Adham)	4		
	Latakia	6		

(Continues)

TABLE 1 (Continued)

Name		Number	Total	Distance of provincial centers from each other	Distance from the administrative centers to Beirut
			Hours	Hours	Hours
	Wadi Qandil		4	12	60
	Main border, Urdukoy		8		
Distance of localities in the South from the Seat in Beirut					
From Saida to Deir al-Qamar 6 hr From Saida to Jbaʿ 4 hr From Saida to Nabatieh 6 hr From Saida to Jezzine 7 hr	Damur River		4.5	9	9
	Nabi Yunis		1.5		
	Han		2.5		
	Saida		0.5		
From Sur to Hunun 6 hr From Sur to Hula 12 hr	Zahrani estuary		2	9	18
	Hawsli Khan		1		
	Jazireh		0.5		
	Nahr Qasim		3.5		
	Sur		2		
Distances from ʿAkka [Acre] to Jerusalem: Shefa-ʿAmr 3 hr; Nazareth 3 hr; Jenin 6 hr; Nablus 6 hr; Jerusalem 12 hr [Total]−30 [hours] Distances from ʿAkka to Tiberias: Shefa-ʿAmr 3 hr; Safuriyya 2 hr; Qana 1.5 hr; Tiberias 5.5 hr [Total] 12 [hours] [Distances from] ʿAkka to Safed: 9 hr; Jubb-Yusuf 3 hr [Total] 12 hr [Distances from] ʿAkka to Tiberias 9 hr [Distances from] ʿAkka to Nazareth 6 hr	Ras al-ʿAyn		1	9	27
	Ras al-Abyad		1		
	Naqura		1		
	Mushrafa		1.5		
	ʿAkka		4.5		

(Continues)

TABLE 1 (Continued)

Name		Number	Total Hours	Distance of provincial centers from each other Hours	Distance from the administrative centers to Beirut Hours
Distances from Jaffa to Jerusalem Ramla 3 hr Ludd 0.5 hr Abu Ghush 2.5 hr Jerusalem 6 hr [Total] 12 [hours]	Haifa		3	24	51
	ʿAtlit		3		
	Tantura		3		
	Caesarea		3		
	Wharf of Sabura (Alexander River)		3		
	Imam Haled (Umm Khalid/ Netanya)		3		
	Haram ʿAli Ibn ʿAlil		3		
	Jaffa		3		
The distance from Gaza to Hebron 12 hr The distance from Gaza to Jerusalem: Beit Jibrin 9 hr Jerusalem 7 hr [Total] 16 [hours] The distance from Jerusalem to Hebron 6 hr	Village of Yibna		4	12	63
	Sudud [Ashdod]		2		
	Majdal [Ashkelon]		2		
	Gaza		4		
	Deir Balah		2	12	75
	Khan Yunes		2		
	Sheikh Zuweid		2		
	Border of Egypt with the Province of Jerusalem		6		

(Continues)

TABLE 1 (Continued)

Name		Number	Total	Distance of provincial centers from each other	Distance from the administrative centers to Beirut
			Hours	Hours	Hours
Distances from the seat in Beirut to localities to its east					
Calculated as 9 hr because of the heights whereas in terms of the distance it is only 6 hr	Deir al-Qamar (6 hr in terms of the distance, calculated 9 hr due to the heights)		9	12	12
	Kafr Nabrakh		1		
	Baruq		1		
	Main border between ʿArqub and the District of Damascus		1		
The main road from the seat in Beirut to Damascus					
	Khan Husayn		6	26	26
	Khan Marj		8		
	Dimas		8		
	Damascus		4		
		From the seat in Beirut to Choueifat 2.5 hr			
		From the seat in Beirut to Bikfaiya 6 hr			

4 | METHODOLOGY

4.1 | Registration of the map

The original map was scanned at the Ottoman Archive in Istanbul into three parts, measuring 530 × 354.25, 530 × 371.7, and 530 × 439.56 mm. The parts were then aligned to produce a continuous map with no overlapping regions. This process resulted in a single sheet measuring 530 × 1,085.68 mm with a resolution of 300 dpi. Jenny (2006) developed MapAnalyst, a software program that analyzes the planimetric accuracy of historical maps. Nevertheless, for registering and to be consistent with other HGIS implementations on the same platform, we decided to use the ESRI© ArcGIS Pro software. To register the map and apply a modern coordinate reference system (CRS), we pinpointed 113 features that appear on the map (source dataset) and also on a present-day orthophoto of Greater Syria (target dataset). These features served as our linking control points (CPs) between the source and target datasets. Most of these points are cities, villages, and crossroads, but some are merely the mid-points and centroids of polyline and polygon features, respectively, such as river mouths, mountain peaks, and lakes (see Figure 2 and Appendix 1). In the analyses it was preferable to use metric units. For this reason, we selected the projected CRS of the Universal Transverse Mercator (UTM) zone 36 North (WGS84 datum) which meets these criteria (Robinson, 2017). Given that the registration of the map only required rotation and scaling, we applied a first-order polynomial transformation (Zitova & Flusser, 2003) to rectify the map. To evaluate the quality of the registration process, we inspected the total root mean square error (RMSE). This represents a least-squares fitting (LSF) of the averaged horizontal and vertical errors between the CPs on the Saida map (source dataset) and their equivalent linked locations on the present-day orthophoto (target dataset). Equations (1) and (2) provide the formulas for the calculation of the RMSE for each of the CPs and the subsequent evaluation of the total RMSE, respectively:

$$\text{RMSE} = \sqrt{u^2 + v^2} \tag{1}$$

$$\text{Total RMSE} = \sqrt{\frac{\sum_i N\,\text{RMSE}^2}{N}} \tag{2}$$

where u and v are the horizontal and vertical errors of a given CP, respectively, and N is the number of CPs. Accordingly, the total RMSE was 8,759.6 m with a minimum, maximum, mean, and median error of 292.7, 38,196.5, 6,331.5 and 4,315.2 m, respectively. The normal curve presenting the error propagation of all the CPs was skewed to the right. That is, several extreme errors were present which significantly increased the mean value, causing the majority of the errors to be lower than the mean (Figure 3a). Splitting the errors into the horizontal and vertical components revealed that the interquartile range (IQR) of the former was smaller than that of the latter, which was associated with the larger extreme errors (Figure 3b). The scatterplot in Figure 3c only indicates a moderate correlation between the horizontal and vertical errors ($R^2 = .36$, $p < .001$). This may be the result of the strong N–S elongation of the map, although a large vertical error does not necessarily imply an equivalently large horizontal error. There were, however, a few regions with apparent inaccuracies, such as the area surrounding Jerusalem and the route segments between Acre and Jaffa.

Naturally, extreme errors increase the total RMSE value, which might lead to a less accurate registration of the map. Thus, to increase the accuracy of registration, extreme outliers can be excluded provided that enough CPs which are spatially distributed all over the map are left to complete the registration process. For this purpose, the 113 CP errors were categorized into quartiles, and the errors (CPs) associated with the fourth quartile were omitted (Appendix 1). Once these outliers were removed, the remaining 84 CPs were used to re-register the map and rectify a version that was much more accurate than the one using all the CPs. Accordingly, the total RMSE decreased to 3,928.3 m, with minimum, maximum, mean, and median errors of 292.7, 7,616.8, 3,578.2 and 3,200.1 m, respectively. The normal curve of the error propagation following this step (Figure 3d) was much less skewed than the curve generated using all the CPs (Figure 3a), and the errors were spread more equally below and above the mean value.

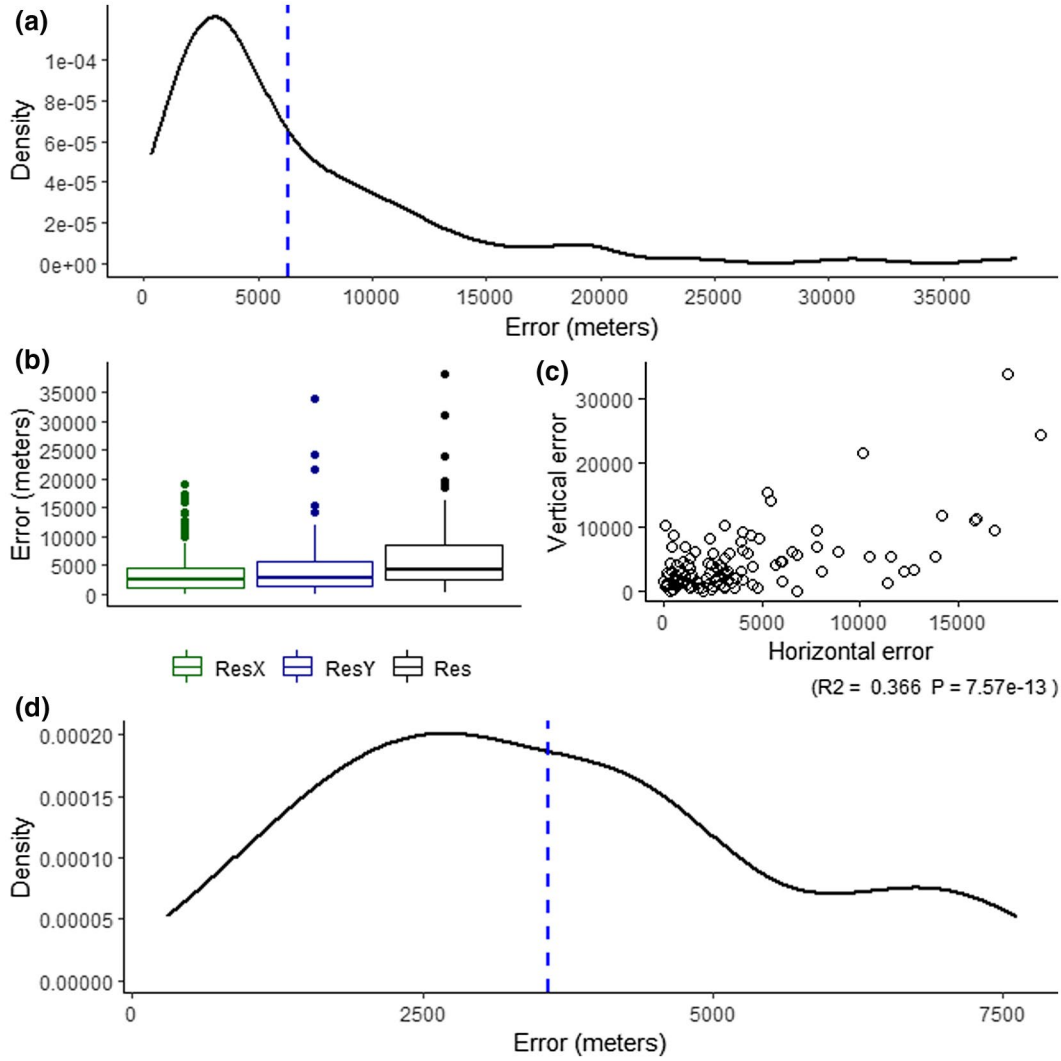

FIGURE 3 Error distribution of the map. (a) The error propagation of all 113 CPs (see also Appendix 1). The mean value is denoted by the vertical dashed blue line. (b) Boxplots of the errors grouped by the horizontal (ResX), vertical (ResY), and combined errors (Res) denoted in green, blue, and black, respectively. (c) Scatterplot of the horizontal errors vs. the vertical errors (correlation coefficient $R = .36$, $p < .001$). (d) The error propagation of the 84 CPs that belong to the first to third quartiles. The mean value is denoted by the vertical dashed blue line

4.2 | Digitization of map route segments

Once the map was registered and its accuracy evaluated, we digitized the network of route segments portrayed on the map and listed in the embedded table (Figure 2). Each of the segments was assigned its corresponding travel time (in hours) between the start and end locations (Table 1). The digitized segments were then grouped into 10 major routes (Table 2). Most of the localities and segments portrayed on the map were synchronized with the table. However, there were four types of inconsistencies: (1) segments that appeared in the table but were not portrayed in the map (e.g., the route from Gaza to Jerusalem via Bet Jibrin or the route from Saida to Nabatieh);

TABLE 2 The segments corresponding to the 26 routes as inferred from the Saida map and the travel timetable (Figure 2), compared to the equivalent segments reconstructed by LCP analyses. Columns indicate **Type**—coastal (C) or inland (I); **Reg**—1 (north of Beirut), 2 (segments between Acre and Beirut), and 3 (south of Acre); **D_M**—length (distance) of the map segments (km); **T_M**—travel times for map segments (h); **D_LCP**—length (distance) of the LCP segments (km); **T_LCP**—travel time of the LCP segments (h); **D_Diff**—the difference in length between D_M and D_LCP; **T_Diff**—the travel time difference between T_M and T_LCP; **Notes**—notes, comments, and remarks. The absolute outlier values of D_Diff and T_Diff belonging to the fourth quartile of each parameter's distribution are bolded in red

Id	Route segments	Type	Reg.	D_M (km)	D_LCP	T_M (h)	T_LCP (h)	D_Diff	T_Diff	Notes
1	Beirut–River mouth (Beirut)	C	1	2.9	6.1	0.5	1	3.2	0.5	The midway location of the Al-Abrash River (as listed in the travel timetable) could not be identified. Thus, the two adjoining segments were amalgamated to a single segment (Al-Kabir River–Arab Jaish).
	River mouth (Beirut)–Deir Mar Elias	C	1	4.2	18.6	1	3.8	**14.4**	**2.8**	
	Deir Mar Elias–al-Kalb River	C	1	6.8	20.9	1	4.2	**14.1**	**3.2**	
	Al-Kalb River–Jounieh	C	1	4.4	4.1	1.5	0.7	−0.3	−0.8	
	Jounieh–Maʿamaltein	C	1	5.6	2.9	1	0.5	−2.7	−0.5	
	Maʿamaltein–Tabarja	C	1	6.7	4	1	0.7	−2.7	−0.3	
	Tabarja–Ibrahim River	C	1	7.7	4.5	0.5	0.7	−3.2	0.2	
	Ibrahim River–Biblos (Jbeil)	C	1	8.3	6.4	1.5	1	−1.9	−0.5	
	Biblos (Jbeil)–Batroun	C	1	19.6	16.7	4	2.7	−2.9	−1.3	
	Batroun–Chekka	C	1	8.8	11.1	2	1.9	2.3	−0.1	
	Chekka–al-Qalamoun	C	1	10	9.1	3	1.5	−0.9	−1.5	
	Al-Qalamoun–Trablus (Tripoli)	C	1	6	7.1	1	1.1	1.1	0.1	
	Trablus (Tripoli)–al-Barid River	C	1	13.8	14.7	2	2.3	0.9	0.3	
	Al-Barid River–al-Kabir River	C	1	20.8	16.3	4	2.6	−4.5	−1.4	
	Al-Kabir River–Arab Jaish	C	1	10.8	22.2	3	3.7	**11.4**	0.7	
	Arab Jaish–Tartus	C	1	12.5	37.1	3	6	**24.6**	**3**	
	Tartus–al-Marqab	C	1	30.2	30.6	6	5.3	0.4	−0.7	
	al-Marqab–Baniyas	C	1	7.7	4	2	0.7	−3.7	−1.3	
	Baniyas–Jablah	C	1	17.1	21.4	4	3.4	4.3	−0.6	
	Jablah–Latakiah	C	1	25.7	23.4	6	3.8	−2.3	**−2.2**	
	Latakiah–Wadi Qandil	C	1	22.3	24.3	4	4	2	0	
	Wadi Qandil–Urdukoy	C	1	27.2		8				

(Continues)

TABLE 2 (Continued)

Id	Route segments	Type	Reg.	D_M (km)	D_LCP	T_M (h)	T_LCP (h)	D_Diff	T_Diff	Notes
11	Tripoli–Safita	I	1		55.6	12	9.2		−2.8	
12	Tripoli–Jisr al-Aboul	I	1			12				No identification of the route.
13	Tripoli–Akkar	I	1		38.1	9	6.6		−2.4	
14	Tripoli–Dannieh (Sir al-Dannieh)	I	1		20.3	6	4.2		−1.8	
15	Latakiah–Jabal al-Akrad	I	1		51.7	12	9.4		−2.6	
16	Latakiah–Bujak	I	1			8				No identification of the route.
17	Latakiah–Bahlouliah	I	1		19.7	6	3.4		−2.6	
18	Latakiah–Sahbun	I	1			6				No identification of the route.
19	Latakiah–Saruja	I	1			12				No identification of the route.
2	Beirut–Damour River	C	2	12.6	22.9	4.5	3.7	10.3	−0.8	The Sarafand–Jezireh (5.2 km, 0.5 hr) and Jezireh–Qasim River (4.7 km, 3.5 hr) segments make no sense in terms of length versus. travel time. Instead, we used the Sarafand–Qasim River segment as an alternative.
	Damoun River–Nabi Younes	C	2	5.9	5.7	1.5	1	−0.2	−0.5	
	Nabi Younes–Chan	C	2	13.8	11.5	2.5	2	−2.3	−0.5	
	Chan–Saida	C	2	2.8	2.4	0.5	0.4	−0.4	−0.1	
	Saida–Zaharany	C	2	5.7	3.1	2	0.5	−2.6	−1.5	
	Zahrani–Sarafand (Hawsli Khan)	C	2	2.9	12.3	1	2	9.4	1	
	Sarafand (Hawsli Khan)–Qasim River	C	2	9.7	14.1	4	2.3	4.4	−1.7	
	Qasim River–Tyre	C	2	10.6	9.7	2	1.6	−0.9	−0.4	
	Tyre–Ras al-ʿAin	C	2	5.8	5.8	1	0.9	0	−0.1	
	Ras al-ʿAin–Ras al-Abyad	C	2	6.9	9.8	1	1.6	2.9	0.6	
	Ras al-Abyad–Naqura	C	2	10.4	10	1	1.7	−0.4	0.7	
	Naqura–Mushrafa	C	2	8.4	1.2	1.5	0.2	−7.2	−1.3	
	Mushrafa–Acre	C	2	14.1	19.3	4.5	3	5.2	−1.5	
	Acre–Haifa	C	3	18.2	19	3	3	0.8	0	
	Haifa–ʿAtlit	C	3	18.7	17.6	3	3	−1.1	0	
	ʿAtlit–Tantura	C	3	10.1	6.2	3	1	−3.9	−2	

(Continues)

TABLE 2 (Continued)

Id	Route segments	Type	Reg.	D_M (km)	D_LCP	T_M (h)	T_LCP (h)	D_Diff	T_Diff	Notes
	Tantura–Caesarea	C	3	13	16.7	3	2.7	3.7	−0.3	
	Caesarea–Wharf of Sabura	C	3	11	12.7	3	2	1.7	−1	
	Wharf of Sabura–Imam Khaled	C	3	12.2	7.5	3	1.2	−4.7	−1.8	
	Imam Khaled–Haram ʿAli	C	3	14.9	17.4	3	2.8	2.5	−0.2	
	Haram ʿAli–Jaffa	C	3	24.9	17.2	3	2.8	**−7.7**	0.2	
21	Saida–Deir al-Qamar	I	2		26.8	6	5.3		−0.7	1. Tyre–Hunun and Tyre–Hula not portrayed on the map but described in the table. 2. The southern location of the Hula lake was selected (there is another route between Tyre and Jahula [45.3 km, 8.1 hr]).
22	Saida–Jba	I	2		17.1	4	3.6		−0.4	
23	Saida–Nabatieh	I	2		25.6	6	4.7		−1.3	
24	Saida–Jezzine	I	2		22.1	7	4.6		**−2.4**	
25	Tyre–Hunun	I	2		37	6	6.7		0.7	
26	Tyre–Hula south	I	2		51.9	12	9.1		**−2.9**	
3	Jaffa–Village of Yibna	C	3	23.8	20.9	4	3.4	−2.9	−0.6	El-ʿArish is closest to the border between Egypt and the Jerusalem province.
	Village of Yibna–Sudud	C	3	14.1	15.7	2	2.5	1.6	0.5	
	Sudud–al-Majdal	C	3	18.4	12.5	2	2	**−5.9**	0	
	Al-Majdal–Gaza	C	3	25	22.9	4	3.7	−2.1	−0.3	
	Gaza–Deir al-Balakh	C	3	9.1	14.6	2	2.3	5.5	0.3	
	Deir al-Balakh–Khan Younes	C	3	12.1	9.9	2	1.6	−2.2	−0.4	
	Khan Younes–Sheikh Zuweid	C	3	8.9	24.3	2	3.9	**15.4**	**1.9**	
	Sheikh Zuweid–El-ʿArish	C	3	19.3	33.2	6	5.3	**13.9**	−0.7	
4	Jaffa–Ramla	I	3	23.6	18.8	3	3	−4.8	0	The route as indicated in the table makes no sense: (1) going through Lod; (2) not going through Latrun; (3) the numbers for Abu Gosh (travel and time) are more appropriate for Latrun (see the Ludd–Latrun and Latrun–Jerusalem) segments. 2. Ludd–Latrun (16.9 km, 2.8 hr); Latrun–Jerusalem (26.5 km, 4.9 hr).
	Ramla–Ludd	I	3	4.6	4.9	0.5	0.75	0.3	0.2	
	Ludd–Abu Gosh	I	3	12.9	27.3	2.5	5	**14.4**	**2.5**	
	Abu Gosh–Jerusalem	I	3	24.2	13.4	6	2.4	**−10.8**	**−3.6**	

(Continues)

TABLE 2 (Continued)

Id	Route segments	Type	Reg.	D_M (km)	D_LCP	T_M (h)	T_LCP (h)	D_Diff	T_Diff	Notes
5	Gaza–Hebron	I	3	74	64	12	11.3	**−10**	−0.7	The map segment goes through Beersheba but the map time is not indicated. The opposite direction Hebron–Gaza is 64.3 km and 10.7 hr.
	Jerusalem–Hebron	I	3	34.5	34	6	5.9	−0.5	−0.1	The map segment goes through Bet Lehem but the map time is not indicated. The opposite direction Hebron–Jerusalem is 34.1 km, 5.8 hr.
51	Gaza–Bet Jibrin	I	3		46	9	7.6		−1.4	Route not mapped (appears in the table but not on the map).
52	Jibrin–Jerusalem	I	3		41	7	7.4		0.4	
6	Acre–Shefa-'Amr	I	3	16.3	17.5	3	2.9	1.2	−0.1	Jenin–Sannur (13.7 km, 2.4 hr), Sannur–Nablus (18.4 km, 3.5 hr).
	Shefa-'Amr–Nazareth	I	3	23.9	17	3	3.1	**−6.9**	0.1	
	Nazareth–Jenin	I	3	23.8	27.6	6	4.5	3.8	−1.5	
	Jenin–Nablus	I	3	28.9	29.6	6	5.6	0.7	−0.4	
	Nablus–Jerusalem	I	3	65.5	55.6	12	9.7	**−9.9**	**−2.3**	
7	Acre–Shefa-'Amr	I	3	16.3	17.5	3	2.9	1.2	−0.1	
	Shefa-'Amr–Sepphoris	I	3	13	12.7	2	2.2	−0.3	0.2	
	Sepphoris–Kana	I	3	8.3	5.8	1.5	1	−2.5	−0.5	
	Kana–Tiberias	I	3	19.5	21.2	5.5	3.5	1.7	**−2**	
71	Acre–Tiberias	I	3		51.1	9	8.5		−0.5	Not portrayed on the map but mentioned as a "direct route?" Note that the "direct route from Acre to Tiberias is indicated on the Saida map as 9 hr whereas the route via Sepphoris and Qana to Tiberias is 12 hr.
72	Acre–Nazareth	I	3		34.4	9	5.9		**−3.1**	
8	Acre–Safed	I	3	43.2	43.8	9	8	0.6	−1	The Safed–Jubat Yousef segment is not portrayed on the map.
	Safed–Jubat Yousef	I	3		6.6	3	1.1		**−1.9**	

(Continues)

TABLE 2 (Continued)

Id	Route segments	Type	Reg.	D_M (km)	D_LCP	T_M (h)	T_LCP (h)	D_Diff	T_Diff	Notes
9	Beirut–Choueifat	I	2	10.1	11	2.5	1.9	0.9	−0.6	1. The route to Deir al-Qamar is indicated as including "Choueifat" and "Bikfaiya." The latter is probably a mistake since its true location is about 12 km to the north. This gives 2.5 hr to Choueifat and 6.5 hr from there to Deir al-Qamar. 2. Kafr Nabrakh is not portrayed on the map and only appears in the travel table. The Deir al-Qamar–Baruq route is 12.4 km (hence the Deir al-Qamar–Nabrakh was divided into two segments of 1 hr each). 3. The location of the "main border between Arqub and the district of Damascus" is approximated.
	Choueifat–Deir al-Qamar	I	2	9.7	15.8	6.5	3.8	6.1	−2.7	
	Deir al-Qamar–Kafer Nabrakh	I	2	6.2	7	1	1.4	0.8	0.4	
	Kafr Nabrakh–Baruq	I	2	6.2	5.2	1	1	−1	0	
	Baruq–Main border between ʿArqub and the District of Damascus	I	2	8.2	14.2	1	3.1	6	2.1	
91	Beirut–Bikfiah	I	2		20.7	6	4.1		−1.9	The location of Bukfiah is wrong and there is no route depicted on the Saida map.
10	Beirut–Khan Marj	I	2	45.5	44.5	14	8.4	−1	−5.6	Khan Husayn was not identified; thus, the segment was evaluated between Beirut to Khan Marj: Beirut–Khan Hussay (19.8 km, 6 hr); Khan Hussay–Khan Marj (25.7 km, 8 hr).
	Khan Marj–Dimas	I	2	31.7	31.4	8	5.4	−0.3	−2.6	
	Dimas–Damascus	I	2	25.5	23.2	4	3.8	−2.3	−0.2	
	N			74	91	96	91	74	91	
Statistics of the **absolute** values:										
	Min			2.8	1.2	0.5	0.2	0	0.0	
	1Q			8.3	9.8	2.0	1.6	1	0.3	
	2Q			12.6	17.4	3.0	3.0	2.5	0.7	
	3Q			21.6	24.9	6.0	4.6	5.4	1.9	
	Max			74.0	64	14.0	11.3	24.6	5.6	
	Average			16.2	20.1	4.4	3.5	4.2	1.1	

(2) segments that were only partially portrayed (e.g., the route from Safed to Jubbat Yousef or from Latakiah to Urdukoy); (3) segments that were portrayed on the map but not listed in the table (e.g., from Safed to Bnot Yaʿakov Bridge); and (4) localities that were listed in the table but did not appear on the map (e.g., Sahbun or Hunan).

4.3 | Reconstruction of the route segments using the least-cost path

In order to examine the digitized map segments, we reconstructed an equivalent network of segments using least-cost-path (LCP) functions. The underlying assumption of LCP was that a given route in the past was well fitted to the topographical slopes composing the route, in order to save energy or time while traveling from the source to the target locations (Herzog, 2013). In other words, any type of journey will attempt to travel in a least-cost effort path and preferably at the same topographical height. This is applicable to pedestrians, horseback riders, or caravans using pack animals such as camels, mules, and donkeys (e.g., Batten, Clark, & Hagemeister, 2007; Douglas, 1994; Ejstrud, 2005; Zohar & Erickson-Gini, 2020). The LCP-based reconstruction of the route segments could thus implement one of several cost functions. We used the built-in cost functions in the ESRI© ArcGIS Pro software that estimate movement in terms of effort expended (the *cost distance* function) and time (the *path distance* function). Since the map segments are assigned travel times, we selected the path distance function to reconstruct an equivalent network.

Basically, the function requires two inputs. The first is a digital elevation model (DEM) of the surface between the source and target locations. We used the Japanese ALOS-PALSAR DEM (JAXA, 2021) downloaded from EARTHDATA (https://search.asf.alaska.edu/#/), with a resolution of 12.5 m/pixel. Like other satellite-based data of the Earth's geoid, the PALSAR data may be biased (Shimada, 2010) but because of our relatively large study area, the potential distortions were trivial. The downloaded tiles of the DEM were mosaicked together into a single surface and clipped to the area under investigation, resulting in a dataset with minimum and maximum values of −414 and 3,115 m, respectively. Then, we assigned a "NoData" value to bodies of water such as the Mediterranean Sea, the Dead Sea, and the Sea of Galilee and used the *focal statistics* and *fill* functions to fill sinks lower than 10 m between a given raster cell and its surrounding neighborhood.[3] The second input of the path distance function is the walking velocity along a sloped surface. It corresponds to the time needed to travel a unit of distance at a given slope. Obviously, it is easier to walk along a flat surface, whereas velocity is likely to decrease as the slope gets steeper. To define the velocities for slopes between −70 and 70°, we used the hiking function developed by Tobler (1993):

$$W = 6^{-3.5 * |(S + 0.05)|} \tag{3}$$

where W is the hiking velocity (km/hr) and S is the degree of slope.[4] For example, for 0° (flat) and 10° slopes, the velocities are 5.036 and 2.71 km/hr, respectively. These velocities correspond to traveling by foot, which is obviously slower than on horseback, and thus were multiplied by 1.25 (Irmischer & Clarke, 2018; Tobler, 1993). Note, however, that the travel time between the source and target locations may be different when traveling in the opposite direction (the way back from the target to the source location). In other words, traveling uphill and downhill on the same path is likely to be different in terms of effort expended and time. The Tobler function takes this into consideration and thus yields different velocities for similar negative and positive slopes.

Using the DEM and the calculated velocities as inputs to the path distance function, we reconstructed the LCP of each of the segments listed in the travel times table on the map (Table 1). Since the map is less accurate than modern maps and present-day orthophotos, the reconstruction used the present-day source and target locations (instead of the map locations). However, since the topography has not changed dramatically in the last 170 years, we could estimate whether the path, the lengths, and the travel times for which the route segments were initially

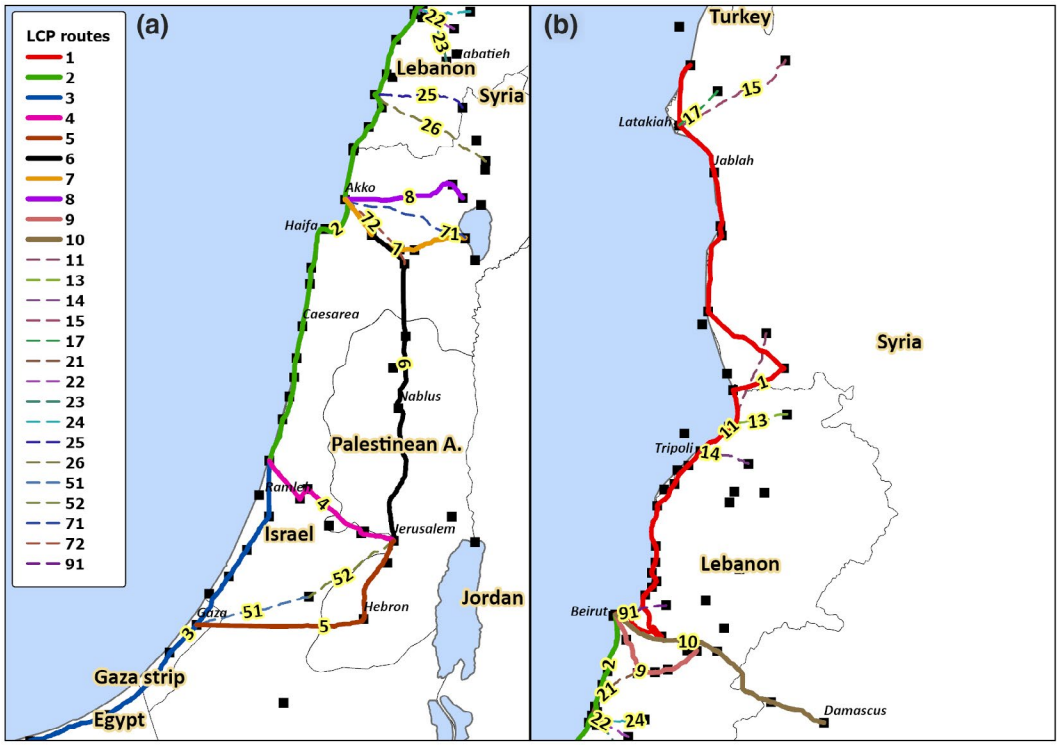

FIGURE 4 Segments grouped into routes as reconstructed by LCP analyses. (a) The southern part of the study area (present-day Egypt, Israel, Gaza and the West Bank and southern Lebanon). (b) The northern part of the study area (present-day northern Lebanon, Syria, and southern Turkey). For further details on the route segments, see also Table 2

established were consistent with the topographical principles of the conservation of effort and time. Finally, we compared the length and travel durations of the map segments to their equivalent LCP-based segments.

5 | RESULTS

Both networks were composed of 10 verified routes containing segments portrayed in the Saida map as well as in the travel timetable (routes 1–10; Figure 4 and Table 2). The LCP-based network ended up being larger than the map network because it contains 16 other routes that were partly portrayed on the map or appeared only in the travel timetable (routes 11, 13–15, 17, 21–26, 51, 71–72, and 91; Figure 4 and Table 2). Altogether, there were 26 routes segmented into 96 parts (Figure 4 and Table 2). Four other routes could not be identified (routes 12, 16, 18, and 19; Table 2) and a single segment belonging to route 1 was vague (the segment from "Wadi Qandil" to "Urdukoy"). The completeness of the routes differed; namely, the coastal routes from El-ʿArish in the south to Latakia in the north were complete, whereas the inland routes only covered those from the coastal settlements.

The details of the map and the LCP-based segments in terms of length (km) and travel time (h) are presented in Table 2. The minimum, median, maximum, and average lengths of the map segments were 2.8, 12.6, 74, and 16.2 km, respectively, and for the travel times were 0.5, 3, 14, and 4.4 hr, respectively. The same statistics for the travel time of the LCP-based segments were 0.2, 3, 11.3, and 3.5 hr, respectively. When subtracting the lengths of the map segments from those of the equivalent LCP-based segments (D_LCP – D_M = D_Diff, Table 2), the

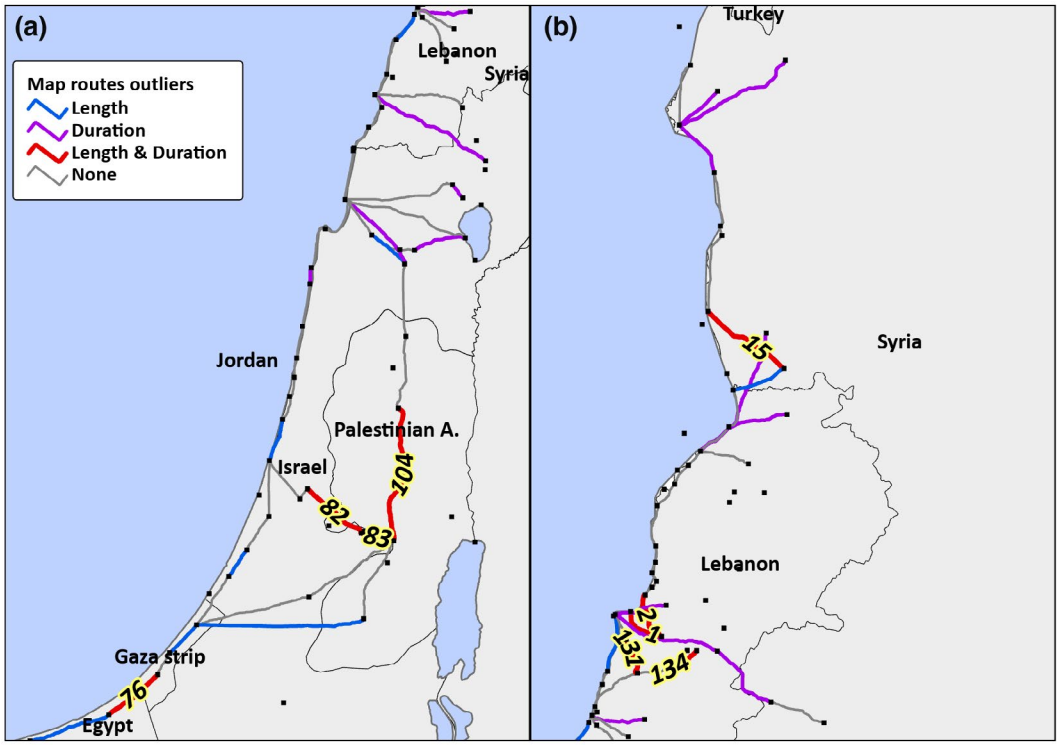

FIGURE 5 The route segments categorized by segments with large outliers for length differences, travel time differences, and both

resulting absolute minimum, median, maximum, and average difference values were 0, 2.5, 24.6, and 4.2 km, respectively. A similar subtraction of the map segment travel times from the LCP-based equivalent segments (T_LCP – T_M = T_Diff, Table 2) yielded minimum, median, maximum, and average difference values of 0, 0.7, 5.6, and 1.1 hr, respectively.

Figure 5 presents the spatial distribution of the outliers for the length difference (D_Diff) and travel time difference (T_Diff) parameters. These outliers are the segments that belong to the fourth quartile of the absolute values of each of the two parameters (Table 2). Nine segments had large differences in both length and travel times, and 10 and 14 had large length and travel time differences, respectively.

The distributions of the length difference (D_Diff) and the travel time difference (T_Diff) parameters are presented in Figure 6. The histogram shows that most of the travel time differences were negative (i.e., the Ottoman estimations of the travel times were longer than the times emerging from the LCP-based reconstruction). This may suggest that some of these estimations were not directly experienced or ridden, but rather were compiled by the cartographer(s) based on information gleaned from travelers. In contrast, the length differences appeared to be more equally distributed around zero (with a few prominent positive outliers).

6 | DISCUSSION

The total RMSE of the Saida map was 3,928.3 m, excluding outliers belonging to the fourth quartile of the CP distributions (Appendix 1). However, given that the Saida map does not contain a scale bar, coordinates, or other reference scales, it is impossible to determine the level of accuracy on the map canvas itself. Nonetheless, it is obvious that the map does not meet modern standards of cartography (Kimerling, Muehrcke, Muehrcke, &

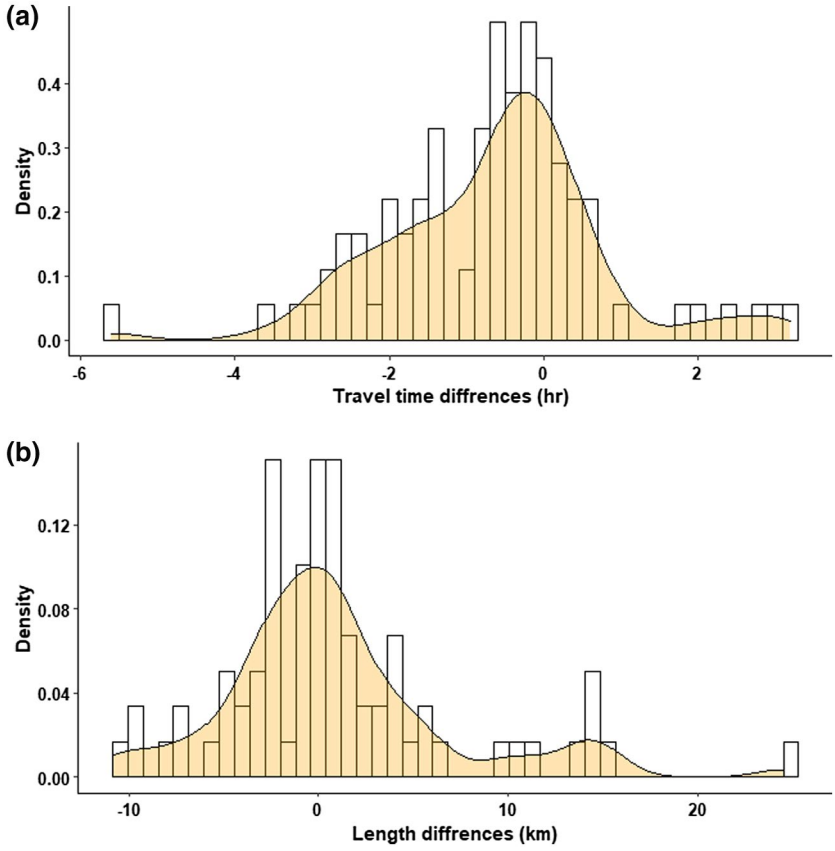

FIGURE 6 (a) Histogram of the travel time differences (LCP time—map time). (b) Histogram of the length differences (LCP length—map length)

Muehrcke, 2016; Minnesota Planning, 1999). The map contains routes, administrative centers, settlements, bodies of water, and major rivers. It is not as inclusive or accurate as other contemporary British maps, such as the 1881 Palestine Exploration Fund (PEF) map (RMSE = 74.4 m; Levin, 2006), the 1915 Newcomb map (RMSE = 100.3 m; Zohar, 2019), German maps (e.g., by Berghaus and Kiepert) and Dutch maps by Van de Velde (Schelhaas et al., 2017), or even the early 19th-century French map by Jacotin (Karmon, 1960). However, in general, the map does not appear to differ from other contemporary Ottoman maps that do not meet the professional standards of their European counterparts, although the Ottoman army gradually commissioned modern up-do-date cartographic maps during the latter half of the 19th century (Ben-Bassat & Ben-Artzi, 2018). The coastal routes seem to be complete, as opposed to the omission of some important inland routes whose inclusion in the map would have made it more accurate. These include the long international route from the Indian Ocean via the Hejaz to Damascus and Aleppo (the latter was also the storage depot for merchandise from Iran), the local trading route connecting the Syrian coast with Egypt, and the new route from the immediate coastal region via Acre where raw materials were exported to France (Philipp, 1998). The absence of these important routes from the map may be suggestive of regions that the Ottoman government was less interested in at the time, and those for which it had no immediate aspirations to exert its power and control. Occasionally, maps are subjected to the prevailing geopolitical situation (Edney, 2009; Harley, 2009; Withers, 2013) and the Saida map may be no exception in this regard. In fact, the Ottoman dominance was precarious at the time in these regions, probably as a result of the Egyptian occupation and the rise of powerful elements in several remote mountainous areas, which were only subdued in the 1850s–1860s (e.g., ʿAqil Agha in Galilee, the Abu-Gosh family near Jerusalem, and others)

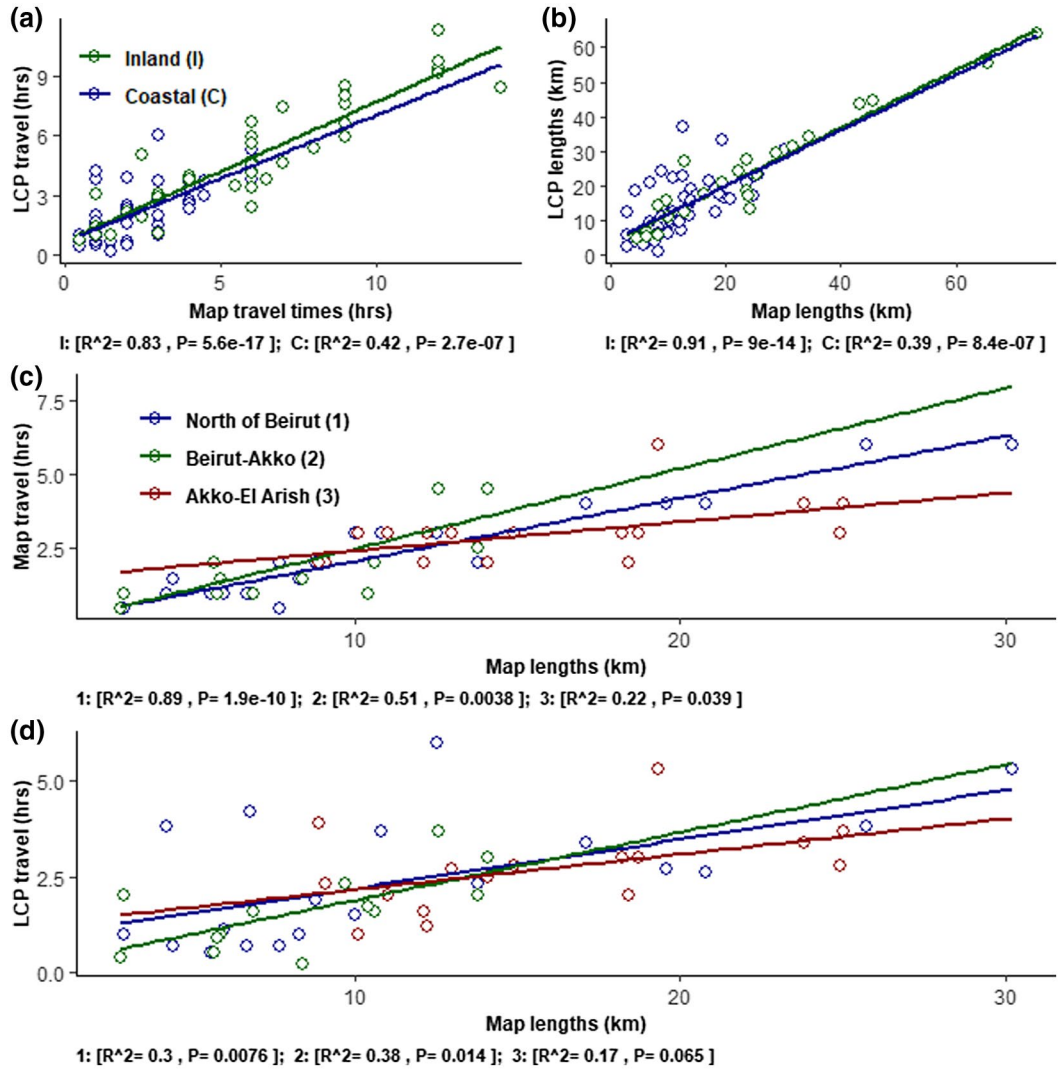

FIGURE 7 (a) The correlation between map travel times and LCP-based travel times classified into inland segments (in green, labeled "I") and coastal segments (in blue, labeled "C"). (b) The correlation between map lengths and LCP-based lengths classified into inland and coastal segments. Same legend and labels as (a). (c) The correlation between map length and map travel times in the coastal segments, classified into three regions: (1) north of Beirut (noted in blue); (2) between Beirut and Acre (green); and (3) between Acre and El-ʿArish (red). (d) The correlation between the map lengths and LCP travel times (same classification as in c)

(Schölch, 1993). This is also supported by Doumani's (1994) suggestion that after the defeat of the Egyptian army in 1840, economic activity in Greater Syria gradually shifted from inland to the coastal cities.

The map depicts the network of routes connecting the administrative centers with other settlements and the travel times between localities (Figure 2). The coastal routes on the map were more complete than the inland ones. Figure 6 shows that their lengths were estimated by the cartographer(s) more consistently than the travel times. Figure 7 categorizes the routes into two groups of coastal and inland segments. The correlations between the inland map and LCP segments were R^2 = .83 and .91 for the travel times and lengths, respectively (Figure 7a), whereas for the coastal segments they were R^2 = .42 and .39, respectively (Figure 7b). Since LCP principles were more dominant in the steeper topographies than in the plains, these correlations suggest that the cartographer(s)

were indeed aware of the inland topography and portrayed the routes accordingly. This is also evident in light of the comment concerning the route from Beirut to Deir al-Qamar: "Calculated as 9 hr because of the heights whereas in terms of the distance it is only 6 hr" (Table 1). If they were aware of the topography and used a scale for time travel estimation but still made significant errors in several regions in the map, they may have had little knowledge, experience, or interest in these regions. In contrast, the travel times for several of the inland routes were significantly overestimated in relation to the LCP reconstruction (Table 2 and Figure 5), although at a resolution of 12.5 m of the manipulated DEM, some turns in the paths of the latter may have been simplified or missed. During the LCP reconstructions we used speed on horseback, which is suitable for movement along a flat surface at a given gradient. However, horses travel much more slowly on narrow, curved inland paths. Moreover, in some places, the topography may have been too steep and complex for horses to pass. Many of the inland routes at the time were used by trading caravans drawn by pack animals such as donkeys and mules for commercial purposes (Avitzur, 1968, 1970, 1972; Fawaz, 1998; Philipp, 1998). This is another indication that the cartographer(s) were aware of the actual conditions and took them into consideration when depicting the routes.

The completeness of the coast segments makes it possible to examine the map routes regionally and evaluate the knowledge and experience of the cartographer(s) as a function of the regions of the map. Figure 7c presents the correlations between the lengths portrayed by the cartographer(s) and the estimated travel times. The correlations were evaluated for three groups of segments: (1) segments north of Beirut; (2) between Acre and Beirut; and (3) south of Acre. The correlation was high ($R^2 = .89$, $p < .001$) for the northern region but weaker moving south: for the intermediate and southern regions, the correlations were $R^2 = .51$ and .22, respectively (both non-significant).

The decreasing trajectory heading south may imply less knowledge and interest on the part of the Ottoman government at the time as regards the southern regions of Greater Syria, which may also have influenced the cartographic accuracy and quality of the map. In other words, the greater cartographic inaccuracy of the map's southern regions may imply a lesser sovereignty and familiarity of the Empire with these regions under its rule. A good example is the coastal route from Acre to Jaffa, which the cartographer(s) divided into eight segments. Although the digitized lengths of these segments range from 10.1 to 24.9 km, the travel times for each segment are listed as exactly 3 hr. Since the coast is mostly flat and the topography had little impact, one would expect significant differences in the travel times for each segment, as calculated for the other northern coastal routes. At the time there was no good route between Haifa and Jaffa, which went through vast expanses of wetlands (Levin, Elron, & Gasith, 2009). Since the trails were in bad condition and subjected to winter precipitation, most movement was maritime. The equal travel times provided by the cartographer(s) are thus indicative of the vague information at their disposal on this part of the route and are consistent with written sources indicating that maritime transportation—rather than riding or caravans—was the most common form of travel between these settlements (Qatinqa, 1961). The correlations between the map length and the LCP travel times in the coastal segments (Figure 7d) lend weight to this assumption, since the correlations for the three regions were substantially lower. That is, the cartographer(s) presumably made their travel estimations based on the map lengths.

Two routes deserve special attention. The first is the Beirut–Damascus road, which was built in the 1850s (Fawaz, 1998). It is likely that the map of the Province of Saida was drawn to correspond to plans to construct routes in the province that required basic information about travel times and distances. For example, the road between Beirut and Damascus was constructed between 1857 and 1862 by the retired French naval officer and entrepreneur Edmond de Perthuis, after considerable deliberations and negotiations. The company he established, *La Compagnie Impériale Ottomane de la Route de Beyrouth à Damas*, was awarded a 50-year lease to operate the road and a monopoly over all wagon transportation using it. This 110 km-long wagon road had to cut through two very high mountain ranges (Lebanon and Anti-Lebanon) and pass through difficult terrain (Fawaz, 1998). The finished road connected the Syrian coast to the interior, boosted economic activity, and enhanced the movement of people and goods between Damascus and Beirut. Beirut, however, emerged as the main beneficiary, since the road strengthened its role as the main port in Greater Syria (Fawaz, 1984, 1998). Interestingly, Damascus and several other locations along the Beirut–Damascus road are the only locations indicated on the map outside the

borders of the Province of Saida. This lends weight to the claim that the drawing of the map was related to the plan to construct the road between Beirut and Damascus. The fact that other roads leading from the coast to the interior in the southern region of the province are much less accurate, and their portrayal includes gross errors in the locations of villages along the road and the orientation of the road, suggests that the cartographer(s) were unfamiliar with the region and did not have accurate information. One good example is the route from Jaffa to Jerusalem, which is clearly inaccurate in that the locations of Latrun, Abu-Gosh, and Qaryat al-ʿAnab are portrayed erroneously in comparison to their present locations, which demonstrates a basic lack of familiarity with the region. In addition, the route from Ramla to Abu-Gosh is erroneously marked as going through Lod. Moreover, the cartographer(s)' estimate of a travel time of 6 hr from Abu-Gosh to Jerusalem, in comparison to 2.4 hr for the LCP, also shows insufficient familiarity.

7 | SUMMARY AND CONCLUSION

This study examined the Ottoman 1849 Saida map using an HGIS approach, in one of the first attempts to quantitatively inspect Ottoman cartography of Greater Syria. Based on 84 control points, the total RMSE of the map emerged to be 3,928.3 m; hence the map does not meet modern standards for accuracy. It is not as inclusive as other contemporary maps, and its main feature is the depiction of the network of routes connecting the administrative centers with other settlements in the Province of Saida. Nevertheless, the information on the map provides useful insights into the historical era when it was drawn up, including the level of Ottoman control of Greater Syria at the time, as well as the cartographer(s)' familiarity with the region as a whole.

The analysis of the lengths and travel times of the segments portrayed by the Ottoman cartographer(s), as compared to the equivalent segments reconstructed by LCP implementations, revealed that the cartographer(s) were aware of the inland topography and the potential complexity of the routes when traveling away from the coast and depicted them as such. The cartography of the coastal segments became more accurate and consistent northward along the coast. This may indicate a lesser degree of familiarity and interest of the Ottoman Empire with the southern coast of Greater Syria at the time.

Overall, the inspection of the Saida map provides a good example of how to extract information from old visual sources, despite their inaccuracies in terms of modern standards. They can reveal the inclusiveness, accuracy, and cartographic attributes of the map and shed light on the initial purposes of drawing up the map, as well as the cartographer(s)' knowhow and preferences. Future work would benefit from examining other historical maps of Greater Syria with HGIS tools, in particular Ottoman maps, which are rarely the subject of thorough cartographical research.

ACKNOWLEDGMENTS

We wish to thank Professor Yossi Ben-Artzi from the University of Haifa for reading the text and adding useful and constructive comments.

CONFLICT OF INTEREST

No conflict of interest is present for this article.

DATA AVAILABILITY STATEMENT

The data that supports the findings of this study are available in the supplementary material of this article.

ORCID

Motti Zohar https://orcid.org/0000-0002-6567-7296
Yuval Ben-Bassat https://orcid.org/0000-0002-4607-4246

ENDNOTES

[1] For instance, see BOA, HRT 0432 (a schematic map in Ottoman probably drawn up before 1900 showing plans for railways and tramways in Syria and southeast Anatolia); HRT 1025 (a map in Ottoman of concessions to build a railroad from Acre to Haifa and from Haifa to Damascus, probably dating from the 1890s, which shows the original proposal for a railway line in red which was not implemented, and a newer one in green which was granted "recently" but only goes as far as a point south of the Sea of Galilee); HRT 1769 (a schematic undated map in Ottoman, probably from the early 1890s, depicting railroads and tramways under construction, planned, and for which there were pending concessions in Greater Syria).

[2] Ottoman administrative officials, army officers, postal carriers, etc. traveled on horseback. This suggests that the timetable provided adjacent to the map was given in riding times. By contrast, goods, raw materials, merchandise, and people were transported on donkeys, mules, and camels, depending on the region, the distance traveled, the availability of pack animals, and the cost. Horses were only rarely used for transportation until the last quarter of the 19th century, when carriages became more common, and suitable roads were built. See Avitzur (1968, 1970, 1972).

[3] The "FocalStatistics" function in the ArcGIS raster calculator is found at Con (IsNull ("palsar_utm36n.tif"), FocalStatistics ("palsar_utm36n.tif", NbrRectangle (9,9), "MEAN"), "palsar_utm36n.tif"; the resulting total cells (excluding the "NoData" cells) were 704,995,415, whereas the number of altered cells after the *fill* function was 39,830,301, which corresponded to 5.64% of the total cells with a mean correction of 1.76 m.

[4] The Excel formula to produce the corresponding velocities for slopes between −70 and 70° is W = 6*(EXP(−3.5*(ABS(TAN(RADIANS(Slope)) + 0.05)))); the outcome is a text file representing the velocities at intervals of 1° (or a tenth of a degree between −10 and 10°). See also http://mapaspects.org/book/export/html/3743/ and http://www.geodyssey.com/papers/tobler93.html.

REFERENCES

Abu-Manneh, B. (1990). Jerusalem in the Tanzimat period: The new Ottoman administration and the notables. *Die Welt Des Islams*, *30*(1), 1–44.

Akarli, E. (1993). *The long peace: Ottoman Lebanon, 1861–1920*. London, UK: The Centre for Lebanese Studies & I.B. Tauris.

Anderson, K. (2019). The hydrographer's narrative: Writing global knowledge in the 1830s. *Journal of Historical Geography*, *63*, 48–60. https://doi.org/10.1016/j.jhg.2018.09.002

Avitzur, S. (1968). *Mi-ukaf le-galgal: Mi-toldot ha-Taḥbura ba-aretz lifnei ha-rekhev hamekhani [From saddle to wheel: About the history of transportation in Eretz-Yisra'el before the mechanical vehicle]*. Tel-Aviv, Israel: Machon Avshalom (Hebrew).

Avitzur, S. (1970). *Me'a shana le-kvish Yafo Yerushalayim [A hundred years to the construction of Jaffa-Jerusalem Road]*. Tel-Aviv, Israel: Machon Avshalom (Hebrew).

Avitzur, S. (1972). *Nemal Yafo: Be-ge'uto uve-shqi'ato, 1865–1965 [The port of Jaffa: During its high days and during its decline, 1865–1965]*. Tel-Aviv, Israel: Milo (Hebrew).

Bailey, T. J., & Schick, J. B. M. (2009). Historical GIS: Enabling the collision of history and geography. *Social Science Computer Review*, *27*(3), 291–296. https://doi.org/10.1177/0894439308329757

Balletti, C., & Guerra, F. (2016). Historical maps for 3D digital city's history. *Cartographica*, *51*(3), 115–126. https://doi.org/10.3138/cart.51.3.3140

Batten, D. C., Clark, J. T., & Hagemeister, E. M. (2007). Least-cost pathways, exchange routes, and settlement patterns in Late Prehistoric east-central New Mexico. In *Proceedings of the 34th Conference of Computer Applications and Quantitative Methods in Archaeology*, Fargo, ND.

Ben-Arieh, Y., & Bartal, I. (1983). *The last phase of Ottoman rule (1799–1917)*. Jerusalem, Israel: Keter (Hebrew).

Ben-Bassat, Y., & Ben-Artzi, Y. (2015). The collision of empires as seen from Istanbul: The border of British-controlled Egypt and Ottoman Palestine as reflected in Ottoman maps. *Journal of Historical Geography*, *50*, 25–36. https://doi.org/10.1016/j.jhg.2015.04.022

Ben-Bassat, Y., & Ben-Artzi, Y. (2016). Cartographical evidence of efforts to develop Acre during the last decades of Ottoman rule. Did the Ottomans neglect the city? *Mediterranean Historical Review*, *31*(1), 65–87. https://doi.org/10.1080/09518967.2016.1173358

Ben-Bassat, Y., & Ben-Artzi, Y. (2018). Ottoman maps of the empire's Arab provinces, 1850s to the First World War. *Imago Mundi*, *70*(2), 199–211. https://doi.org/10.1080/03085694.2018.1450544

Ben-Bassat, Y., & Ben-Artzi, Y. (2019). New cartographical evidence on the efforts to survey Sultan Abdülhamid's lands in northern Palestine at the end of the 19th century. *The New East*, *58*, 65–89 (Hebrew).

Bender, O., Boehmer, H. J., Jens, D., & Schumacher, K. P. (2005). Using GIS to analyse long-term cultural landscape change in Southern Germany. *Landscape and Urban Planning*, *70*(1–2), 111–125. https://doi.org/10.1016/j.landurbplan.2003.10.008

Buessow, J. (2011). *Hamidian Palestine: Politics and society in the District of Jerusalem, 1872–1908*. Leiden, the Netherlands: Brill.

Cooper, D., & Gregory, I. N. (2011). Mapping the English Lake District: A literary GIS. *Transactions of the Institute of British Geographers*, *36*(1), 89–108. https://doi.org/10.1111/j.1475-5661.2010.00405.x

Davie, F. M., & Frumin, M. (2007). Late 18th century Russian Navy maps and the first 3D visualization of the walled city of Beirut. *e-Perimetron*, *2*(2), 52–65.

Douglas, D. H. (1994). Least-cost path in GIS using an accumulated cost surface and slope lines. *Cartographica*, *31*(3), 37–51. https://doi.org/10.3138/D327-0323-2JUT-016M

Doumani, B. B. (1994). The political economy of population counts in Ottoman Palestine: Nablus, circa 1850. *International Journal of Middle East Studies*, *26*(1), 1–17. https://doi.org/10.1017/S0020743800059730

Duany, M. (2012). The Hula nature reserve as a dialectical response to the Hula drainage project. *Horizons in Geography*, *78*, 64–81 (Hebrew).

Edney, M. H. (2009). *Mapping an empire: The geographical construction of British India, 1765–1843*. Chicago, IL: University of Chicago Press.

Ejstrud, B. (2005). Cost surface analysis and ancient roads: A comparison. In J. F. Berger, F. Bertoncello, F. Braemer, G. Davtian, & M. Gazenbeek (Eds.), *Temps et espaces de l'homme en société: Analyses et modèles spatiaux en archéologie* (pp. 135–140). Quétigny, France: Librairie archéologique.

Fawaz, L. (1984). The city and the mountain. Beirut's political radius in the nineteenth century as revealed in the crisis of 1860. *International Journal of Middle East Studies*, *16*, 489–495.

Fawaz, L. (1998). The Beirut-Damascus road: Connecting the Syrian coast to the interior in the 19th century. In T. Philipp & B. Schaebler (Eds.), *The Syrian land: Processes of integration and fragmentation in Bilad al-Sham, from the 18th to the 20th century* (pp. 19–27). Stuttgart, Germany: Franz Steiner.

Goren, H. (2001). Scientific organizations as agents of change: The Palestine Exploration Fund, the Deutsche Verein zur Erforschung Palästinas and nineteenth-century Palestine. *Journal of Historical Geography*, *27*(2), 153–165. https://doi.org/10.1006/jhge.2001.0295

Gregory, I. N., & Ell, P. S. (2007). *Historical GIS: Technologies, methodologies, and scholarship*. Cambridge, UK: Cambridge University Press.

Gregory, I. N., & Healy, G. R. (2007). Historical GIS: Structuring, mapping and analyzing geographies of the past. *Progress in Human Geography*, *31*(5), 638–653.

Hanssen, J. (2005). *Fin de Siècle Beirut: The making of a provincial capital*. New York, NY: Oxford University Press.

Harley, J. B. (2009). Maps, knowledge, and power. In G. Henderson & M. Waterstone (Eds.), *Geographic thought: A praxis perspective* (pp. 129–148). London, UK: Routledge.

Herzog, I. (2013). Review of least cost analysis of social landscapes. Archeological case studies. *Internet Archaeology*, *34*. https://doi.org/10.11141/ia.34.7

Irmischer, I. J., & Clarke, K. C. (2018). Measuring and modeling the speed of human navigation. *Cartography and Geographic Information Science*, *45*(2), 177–186. https://doi.org/10.1080/15230406.2017.1292150

JAXA. (2021). *About ALOS-PALSAR*. Retrieved from https://www.eorc.jaxa.jp/ALOS/en/about/palsar.htm

Jenny, B. (2006). MapAnalyst: A digital tool for the analysis of the planimetric accuracy of historical maps. *e-Perimetron*, *1*(3), 239–245.

Kark, R. (2004). The lands of the sultan: Newly discovered Ottoman cadastral maps in Palestine. In G. Tolias & D. Loupis (Eds.), *Eastern Mediterranean cartographies* (pp. 197–220). Athens, Greece: Institute for Neohellenic Research, National Hellenic Research Foundation.

Karmon, Y. (1960). An analysis of Jacotin's map of Palestine. *Israel Exploration Journal*, *10*(3), 155–173.

Kimerling, A. J., Muehrcke, P., Muehrcke, J. O., & Muehrcke, P. M. (2016). *Map use: Reading, analysis, interpretation*. Redlands, CA: Esri Press.

Knowles, A. K. (2005). Emerging trends in historical GIS. *Historical Geography*, *33*, 7–13.

Lafreniere, D., & Gilliland, J. (2015). "All the world's a stage": A GIS framework for recreating personal time-space from qualitative and quantitative sources. *Transactions in GIS*, *19*(2), 225–246. https://doi.org/10.1111/tgis.12089

Levin, N. (2006). The Palestine exploration fund map (1871–1877) of the holy land as a tool for analyzing landscape changes: The coastal dunes of Israel as a case study. *Cartographic Journal*, *43*(1), 45–67. http://dx.doi.org/10.1179/000870406x93508

Levin, N., Elron, E., & Gasith, A. (2009). Decline of wetland ecosystems in the coastal plain of Israel during the 20th century: Implications for wetland conservation and management. *Landscape and Urban Planning*, *92*(3), 220–232. https://doi.org/10.1016/j.landurbplan.2009.05.009

Levin, N., Kark, R., & Galilee, E. (2010). Maps and the settlement of southern Palestine, 1799–1948: An historical/GIS analysis. *Journal of Historical Geography*, *36*, 1–18. https://doi.org/10.1016/j.jhg.2009.04.001

Manzano, A. F., Martínez, G. J., & San-Antonio-Gomez, C. (2012). GIS analysis of the accuracy of Tomas Lopez's historical cartography in the Canary Islands (1742–1746). *Scientific Research and Essays*, *7*(2), 199–210.

Máoz, M. (1968). *Ottoman reform in Syria and Palestine, 1840–1861: The impact of the Tanzimat on politics and society*. Oxford, UK: Clarendon Press.

Marom, R. (2018). Ottomanizing the maps of Palestine. Ottoman appropriation of European cartographic knowledge and its utilization for late Ottoman needs. *The New East*, *57*, 19–52 (Hebrew).

Minnesota Planning. (1999). *Positional Accuracy Handbook: Using the National Standard for Spatial Data Accuracy to measure and report geographic data quality*. St. Paul, MN: Minnesota Planning, Land Management Information Center.

Philipp, T. (1998). Highways and sea lanes in southwest Syria in the 18th century. In T. Philipp & B. Schaebler (Eds.), *The Syrian land: Processes of integration and fragmentation in Bilad al-Sham, from the 18th to the 20th century* (pp. 3–17). Stuttgart, Germany: Franz Steiner.

Qatinqa, B. (1961). *Me'az ve-'ad hena [From then until here]*. Jerusalem, Israel: Qiryat Sefer (Hebrew).

Robinson, A. H. (2017). Matching the map projection to the need. In M. Lapaine & E. L. Usery (Eds.), *Choosing a map projection* (pp. 49–115). Cham, Switzerland: Springer.

Schaffer, G., & Levin, N. (2014). Mapping human induced landscape changes in Israel between the end of the 19th century and the beginning of the 21st century. *Journal of Landscape Ecology*, *7*(1), 110–145. http://dx.doi.org/10.2478/jlecol-2014-0012

Schaffer, G., & Levin, N. (2016). Reconstructing nineteenth century landscapes from historical maps—The Survey of Western Palestine as a case study. *Landscape Research*, *41*(3), 360–379. https://doi.org/10.1080/01426397.2015.1078454

Schelhaas, B., Faehndrich, J., & Goren, H. (2017). *Mapping the Holy Land: The foundation of a scientific cartography of Palestine*. London, UK: I.B. Tauris & Co. Ltd.

Schölch, A. (1993). *Palestine in transformation 1856–1882: Studies in social, economic and political development*. Washington, DC: Institute for Palestine Studies.

Shimada, M. (2010). Ortho-rectification and slope correction of SAR data using DEM and its accuracy evaluation. *IEEE Journal of Selected Topics in Applied Earth Observations and Remote Sensing*, *3*(4), 657–671. https://doi.org/10.1109/JSTARS.2010.2072984

Tobler, W. (1993). *Three presentations on geographical analysis and modeling*. Santa Barbara, CA: National Center for Geographic Information and Analysis.

Withers, C. W. J. (2013). On Enlightenment's margins: Geography, imperialism and mapping in Central Asia, c. 1798–c. 1838. *Journal of Historical Geography*, *39*, 3–18. https://doi.org/10.1016/j.jhg.2012.08.018

Zitova, B., & Flusser, J. (2003). Image registration methods: A survey. *Image and Vision Computing*, *21*(11), 977–1000. https://doi.org/10.1016/S0262-8856(03)00137-9

Zohar, M. (2017). A city hit by an earthquake: An HGIS approach to reconstructing the damage in Tiberias (Israel) in 1837. *International Journal of Geographical Information Science*, *31*(1), 81–99. https://doi.org/10.1080/13658816.2016.1188933

Zohar, M. (2019). Follow the road: Historical GIS for evaluating the development of routes in the Negev region during the twentieth century. *Cartography and Geographic Information Science*, *46*(6), 532–546. https://doi.org/10.1080/15230406.2019.1577176

Zohar, M. (2020). Advancing the historical geography of late Ottoman and British Mandate Palestine using GIScience. A review. *Transactions in GIS*, *24*(6), 1464–1481. https://doi.org/10.1111/tgis.12667

Zohar, M., & Erickson-Gini, T. (2020). The "Incense Road" from Petra to Gaza: An analysis using GIS and cost functions. *International Journal of Geographical Information Science*, *34*(2), 292–310. https://doi.org/10.1080/13658816.2019.1669795

How to cite this article: Zohar, M., & Ben-Bassat, Y. (2021). Analyzing routes in Ottoman Greater Syria using historical GIS: The 1849 Saida map. *Transactions in GIS*, 25, 2612–2640. https://doi.org/10.1111/tgis.12788

APPENDIX 1.

The list of control points (CPs) used for the registration of the Saida map. Columns include: CP – the name of the control point; Type—the type of the given control point; Link Id—Id of the given control point; Use—a flag denoting if the control point participates in the registration process: F—false; T—True (altogether 84 True CPs); S_X—longitude coordinate on the source; S_Y—latitude coordinate on the source; T_X—longitude coordinate on the target; T_Y—latitude coordinate on the target; ResX—horizontal error; ResY—vertical error; Res—the registration error. The statistics of the errors of the 84 participating CPs appear at the end of the table

CP	Type	Link Id	Use	S_X	S_Y	T_ X	T_Y	ResX	ResY	Res
El-Arish		1	F	9.5	3.4	576,607.8	3,443,840	−13,882.9	−5,269.9	14,849.5
Latakiah	Major city	2	T	10.6	38.1	752,860.3	3,934,730	−3,611.5	561.3	3,654.9
Damascus	Major city	3	T	18.4	25.1	806,567	3,713,113	−4,528.3	3,884.5	5,966.1
Akko	Major city	4	T	12.2	18.3	693,505.1	3,644,612	452.1	−919.8	1,024.9
Tiberias		5	T	15.3	18.3	738,122.8	3,630,348	3.1	1,443.2	1,443.2
Sheikh Zowaiid		6	T	10.7	4.5	605,824.6	3,453,566	−5,987.6	−4,640.9	7,575.6
Khan Yunes		7	T	11.1	4.9	623,991.9	3,468,423	4,232	5,844	7,215.4
Deir El-Balah		8	T	11.4	5.7	628,418.7	3,476,528	1,005	4,553.9	4,663.5
Gaza	Major city	9	F	11.6	6.3	638,385.4	3,486,899	4,887.1	8,309.7	9,640.3
Bee'r Sheba		10	F	15.1	7.8	670,712	3,457,936	−19,203	−24,380.8	31,035.1
Hebron	Major city	11	F	16.2	8.3	700,415.1	3,489,130	−6,831.1	5,568.7	8,813.3
Dead Sea north		12	T	17.7	11.3	741,749.3	3,517,538	−292.2	17.5	292.7
Jericho		13	T	16.9	11.5	733,073.3	3,526,913	2,277	1,042.8	2,504.4
Bet Lehem		14	T	15.9	9.9	709,249.6	3,509,923	−1,098.1	2,306.2	2,554.3
Jerusalem	Major city	15	T	15.7	10.3	711,612.4	3,518,024	3,006.6	3,677.3	4,749.9
Shikma river		16	T	11.7	7.7	643,095.8	3,498,487	3,053.2	−457.8	3,087.3
El-Majdal		17	T	12.1	7.8	650,375.6	3,504,859	4,051.9	6,449.6	7,616.8
Ashdod		18	T	12.5	8.9	657,081.3	3,514,654	148.2	2,870.8	2,874.6
Village of Yibna		19	T	12.6	9.9	665,266.5	3,527,015	2,316.6	2,829.5	3,656.9
Soreq river		20	T	12.2	10.4	661,614.3	3,535,027	2,678.8	1,531.7	3,085.7
Abu Gosh		21	F	14.1	10.4	699,543.3	3,520,842	12,783.2	−3,360.2	13,217.5
Qiryat Anavim		22	T	15.3	11	700,693	3,521,442	−5,715.2	−4,091.4	7,028.8
Latrun		23	F	13.6	10.6	687,520.5	3,523,610	6,553.9	−6,279.7	9,076.8
Ramleh	Major city	24	T	13.4	10.7	676,767.8	3,533,561	−1,146.9	1,131.6	1611.1
Lod		25	T	13.7	10.9	679,582	3,537,285	−2,882.1	4,178.4	5,076
Jaffa		26	T	12.1	11.2	665,445.4	3,547,763	4,493.1	1,095.8	4,624.8
Nablus	Major city	27	T	15.1	14.2	713,285.1	3,567,196	−3,346.3	−5,933.7	6,812.3
Sannur		28	T	14.3	14.8	711,313.6	3,582,190	2,774.5	−3,305.1	4,315.3
Jenin		29	T	14.6	15.5	716,075.7	3,593,857	168.5	834.8	851.6
Haram Ali Ibn Ali		30	T	12.3	12.5	670,292.9	3,563,037	986.8	−1,201.1	1554.5
Ploleg River		31	T	12.2	13.3	672,892.3	3,571,538	926.1	−2,884.6	3,029.6
Umm Khalid		32	T	12.3	13.5	674,693	3,578,692	1,312.9	572.6	1,432.3
Wharf of Sabura		33	T	12.1	14.3	675,571.6	3,585,834	349.5	−4,398.3	4,412.2

(Continues)

APPENDIX 1. (Continued)

CP	Type	Link Id	Use	S_X	S_Y	T_X	T_Y	ResX	ResY	Res
Caesarea	Major city	34	T	12	15	677,700.4	3,597,660	779.1	−3,111.9	3,207.9
Tantura		35	T	12	15.9	680,455.6	3,613,299	531.5	144.9	550.9
Atlit		36	T	11.9	16.5	680,986.2	3,619,319	429.5	−3,101.7	3,131.3
Haifa	Major city	37	T	12	17.4	686,158.2	3,633,703	−425.2	−258.8	497.8
Sea of Galilee south		38	T	15.7	17.8	741,763.8	3,622,121	161	1,102.5	1,114.2
Nazareth		39	T	14.2	17	715,610.2	3,620,709	−1,224.9	4,130.8	4,308.6
Kafr Kana		40	T	14.3	17.5	719,290.3	3,625,799	−769.9	1,780.4	1939.7
Sepphoris		41	T	13.7	17.5	713,838.8	3,625,962	1,913.6	−617	2010.6
Shefara'm		42	T	13	17.7	703,418.8	3,631,423	1,631.8	−1,519.5	2,229.8
Sea of Galilee north [Region]		43	T	15.5	19.1	744,039.2	3,642,668	566.5	2,152.6	2,225.9
Safed		44	T	14.7	19.3	733,405.4	3,650,039	−245.1	2,634.1	2,645.5
Bnot Yaa'kov bridge		45	T	15.4	20.2	745,528.9	3,655,638	−1,392.6	−742.9	1578.4
Hulla south	Lake	46	T	15.2	20.4	745,697.1	3,658,890	−158.6	−1,399.7	1,408.7
Joubat Yossef		47	F	15	20.4	737,234	3,645,191	−5,261.6	−15,453.6	16,324.8
Jahula		48	T	15.1	21	742,254.5	3,666,496	−3,655.8	−1,929.7	4,133.8
Mushrafa		49	T	12	19.1	696,536.6	3,662,716	2,463.3	4,028.6	4,722
Naqura port		50	T	11.9	19.4	696,541.4	3,663,428	2,447.3	−290.3	2,464.5
Nakura		51	T	12.2	19.7	696,849.1	3,663,786	−2,186.7	−2,003	2,965.4
Ras el Abiad		52	T	12	20.4	702,267.3	3,671,462	3,066.4	−5,164.7	6,006.4
Ras Al-Ain		53	T	12.2	20.8	707,171.1	3,678,798	2,778.1	−2,336.4	3,630
Tyre		54	T	12.2	21.1	704,565.2	3,683,514	−1,052.2	−2,346.1	2,571.2
Nabatiyeh	Major city	55	T	13.7	22.3	731,102.8	3,695,839	−933.4	1,585.8	1,840.1
Nahr Qasim		56	T	12.7	21.6	708,961.2	3,691,091	−6,020.2	1,547.4	6,215.9
Jazireh		57	F	12.5	22.5	711,111.9	3,689,914	−5,418.2	−14,184.9	15,184.4
Sarafand		58	T	12.3	22.9	712,449.7	3,703,829	−2,479.9	−5,920.3	6,418.7
Jbaa		59	T	14	23.3	733,951.9	3,707,918	−6,762.4	108.3	6,763.2
Jezzine		60	F	14.3	24.1	739,975.2	3,714,301	−8,018.5	−3,140.8	8,611.6
Zahrani mouth		61	T	12.4	23.1	719,280.5	3,713,219	2,849.9	992	3,017.6
Zahrani split		62	T	12.5	23	722,172.6	3,712,175	3,401.6	1,192.5	3,604.6
Saida		63	T	12.5	23.4	720,438.9	3,715,838	781.8	−999.4	1,268.8
Chan		64	T	12.6	23.6	722,337.8	3,717,045	−110.9	−881.8	888.8
Nahr Awali		65	T	12.6	23.8	721,531.7	3,719,120	−1,440.2	−1,930.9	2,408.9
Arkoub		66	F	14.2	25.2	734,845.9	3,698,589	−17,525.2	−33,938.8	38,196.5
Al-Dimass		67	T	16.8	25.4	786,907.6	3,720,695	−3,272.7	−1,831	3,750.1
Khan Marj		68	F	14.9	25.3	766,983.7	3,739,609	4,471.2	8,795.5	9,866.7
Zahle		69	T	14.7	26.1	769,459.8	3,748,188	6,007.9	4,599.8	7,566.6
Baruc		70	T	14.2	24.9	753,317.7	3,733,618	2,276.2	4,363.3	4,921.3
Deir el-Qamar		71	T	13.5	24.8	737,326.5	3,731,523	−2,480.9	812.6	2,610.6

(Continues)

APPENDIX 1. (Continued)

CP	Type	Link Id	Use	S_X	S_Y	T_X	T_Y	ResX	ResY	Res
Nabi Younos		72	T	12.8	24.4	724,269.8	3,727,294	−4,000.5	−1,696.5	4,345.4
Nahr Damour		73	T	12.8	24.8	726,263.4	3,732,171	−3,127	−2,543.8	4,031
Schouf	Region	74	F	13.6	25.2	755,783.9	3,739,863	12,235.3	3,127	12,628.6
Deir Mar Elias		75	F	12.9	25.5	746,295.6	3,745,083	11,427.5	1,196.2	11,490
Beirut	Major city	76	T	12.5	25.5	729,085.7	3,753,228	1,047.9	6,981.6	7,059.8
Burg		77	F	12.5	25.3	728,446.6	3,752,677	502.8	8,838.1	8,852.4
Chouifat		78	T	13	25.2	733,160	3,743,846	−1,358	5,147.8	5,323.9
Bykfiah		79	F	13.3	25	747,983.3	3,756,612	10,114.4	21,693.4	23,935.4
River mouth (Beirut)		80	F	12.6	25.6	734,793.4	3,754,315	3,951.4	7,684.5	8,640.9
Nahr al-Kalb		81	F	12.9	26	740,179.4	3,760,452	4,057.4	9,310.1	10,155.8
Jounieh		82	F	13.1	26.2	742,755.8	3,763,356	3,108.6	10,354.3	10,810.9
Maa'meltein		83	F	13.3	26.4	744,411.3	3,765,502	−74.5	10,232.1	10,232.4
Sannine	Region	84	T	14.3	26.8	762,647.8	3,758,494	2,665.1	3,496.5	4,396.4
Jebel Lubnan	Region	85	F	14.2	28.2	775,166.5	3,770,110	10,466.7	−5,468.3	11,809.1
Nahr Ibrahim		86	T	13	27.3	744,019.4	3,772,591	677.7	4,151.9	4,206.8
Tabarja		87	T	13.1	26.8	742,713.9	3,768,649	−378.1	6,961	6,971.3
Biblos		88	T	12.8	27.7	744,127.1	3,778,629	1,379.6	2,644.3	2,982.6
Batroun		89	T	12.9	29	744,679.2	3,793,580	−4,773.8	−511	4,801
Ehden		90	T	14.5	29.7	773,285.1	3,798,671	−2,307.8	2,812.4	3,638.1
Qannubine		91	T	14	29.7	771,478.8	3,794,820	3,173.9	−2,728	4,185.2
Jebel el-Makmel	Region	92	F	14.2	29	784,428.2	3,798,383	15,856.5	10,940.8	19,264.7
Chekka Burj		93	T	12.7	29.5	747,267.1	3,799,686	−1,778.9	−1,321.5	2,216.1
Chekka		94	T	12.9	29.6	751,101.9	3,801,560	−1,741.9	−500.4	1812.3
Ras Nachaste		95	T	12.9	29.8	752,154.9	3,806,800	−930.1	2,092.7	2,290.1
Qalamoun		96	T	13.2	30.2	756,228.3	3,808,569	−3,112.2	−711.4	3,192.5
Tripoli	Major city	97	T	13.3	30.6	760,719.6	3,813,736	−1,978.2	61.2	1979.1
Tripoli [Island]	Island	98	T	12.7	31	754,715.9	3,820,433	−536.4	−2516.3	2,572.9
Akkar	Region	99	F	14.7	31.4	792,841.4	3,827,430	7,758.5	9,427.2	12,209.3
Nahr al Bared		100	T	13.4	31.5	771,272.7	3,822,875	3,912.7	−3,162	5,030.7
Nahr el-Kabir		101	F	13.2	32.7	772,829.4	3,836,483	2,362.3	−8,236	8,568.1
Nahr el Abrash		102	T	13.1	32.9	770,528.2	3,842,581	1,581.3	−6,084.2	6,286.3
Arab Jaysh		103	F	13.3	33.6	791,754.1	3,844,480	15,961.2	−11,424.1	19,628.3
Safita		104	F	14.3	34.5	785,150.4	3,857,606	−8,869.6	−6,259.9	10,856.2
Tartus		105	T	12.5	33.7	763,523.6	3,865,631	−1,304.3	3,487.9	3,723.8
Tartus [Island]	Island	106	T	12.4	33.5	761,346.3	3,860,819	−783.6	1,402.4	1606.5
Marqab		107	T	12.2	35.6	768,700.6	3,893,775	686.3	2,397.4	2,493.7
Banyias		108	T	12.3	36.1	768,139.2	3,897,291	−3,632.4	−446.5	3,659.8
Jablah	Major city	109	T	11.8	37.1	765,830	3,917,173	−3,249.5	3,017.4	4,434.4
Al-Bahlouliyah		110	F	11.7	39.8	767,076.7	3,947,314	−11,563.8	−5430.1	12,775.3
Wadi Qandil		111	F	11.5	39.4	756,998.5	3,956,965	−16,864.6	9,432	19,323

(Continues)

APPENDIX 1. (Continued)

CP	Type	Link Id	Use	S_X	S_Y	T_X	T_Y	ResX	ResY	Res
Jebel el-Akrad	Region	112	F	11.3	40.9	792,239	3,958,783	14,160.6	−11,903.3	18,499
Hanzir Bashi		113	F	10	41	752,855	3,971,265	−7,832	−6,836.1	10,395.8
Bet Guvrin [does not appear in the map]										
Sir Dannieh [does not appear in the map]										
Kfar Nabrakh [does not appear in the map]										
Border [does not appear in the map]										
Hunin Castle [does not appear in the map]										
							Min	3.06372	17.53992	292.7275
							Max	6,762.376	6,981.638	7,616.801
							Mean	2,138.79	2,465.426	3,578.243
							Std	1,609.42	1,781.385	1,893.825
							1Q	783.1588	1,031.976	2,223.473
							2Q	1,846.286	2,122.691	3,200.195
							3Q	3,115.895	3,541.702	4,678.12